Coherent Coupling of Two Quantum Dots Embedded in an Aharonov-Bohm Interferometer

A. W. Holleitner,[1,*] C. R. Decker,[1] H. Qin,[1] K. Eberl,[2] and R. H. Blick[1]

[1]*Center for NanoScience and Sektion Physik, Ludwig-Maximilians-Universität, Geschwister-Scholl-Platz 1,
80539 München, Germany*
[2]*Max-Planck-Institut für Festkörperforschung, Heisenbergstraße 1, 70569 Stuttgart, Germany*

We define two laterally gated small quantum dots with less than 15 electrons in an Aharonov-Bohm geometry in which the coupling between the two dots can be changed. We measure Aharonov-Bohm oscillations for weakly coupled quantum dots. In an intermediate coupling regime we study molecular states of the double dot and extract the magnetic field dependence of the coherently coupled states.

Quantum dots are the perfect experimental tool for investigating phase coherent processes in mesoscopic devices [1,2]. One of the questions which can be considered is the entanglement of fermionic particles, e.g., electrons in a solid state environment. In this work we present an experimental approach allowing one to coherently couple two quantum dots by a tunneling barrier embedded in an Aharonov-Bohm (AB) interferometer [3]. For such a system it is expected that singlet and triplet states have distinct AB phases [4]. Therefore, this setup is a promising candidate for realizing a quantum bit in a solid state device [5]. A further question being addressed in this Letter is whether the coherent coupling of such two quantum dots in the few electron limit can be understood in terms of only two excess electrons, one in each quantum dot, or whether the whole shell structure has to be taken into account.

We first show measurements for the case of weak coupling of the two quantum dots which demonstrate that the device acts as an AB interferometer with two small quantum dots. Second, we focus on coherently coupled states within the double quantum dot, first evidence of which has been found in transport [6] and microwave spectroscopy [7]. Finally, we extract the magnetic field dependence of the coherent coupling of the two quantum dots and compare it to recent theoretical models [8,9].

The device is realized within a two-dimensional electron gas (2DEG) being 90 nm below the surface of an AlGaAs/GaAs heterostructure. At a bath temperature of 4.2 K the electron mobility and density are found to be $\mu = 80 \text{ m}^2/\text{V s}$ and $n_s = 1.7 \times 10^{15} \text{ m}^{-2}$. By electron beam writing and Au evaporation Schottky gates are defined which, under appropriate voltage bias, form two quantum dots [1]. In order to operate the interferometer with a single source/drain contact for both quantum dots the contact regions are patterned by an additional layer as depicted by blue areas in the electron beam micrograph of Fig. 1(a). This 45 nm thick layer is fabricated from a negative resist (calixarene) [10] with a dielectric constant of $\epsilon_{\text{cax}} \sim 7.1$ [11]. Hereby, the areas of the 2DEG which are below the calixarene are significantly less depleted by voltages which are applied to gate$_1$ and gate$_2$ [12,13]. By this, we obtain an experimental setup in which one elec-

tron can either tunnel through dot$_1$ or dot$_2$ [see Fig. 1(b)]. Furthermore, since gate$_1$ and gate$_2$ form a tunable tunneling barrier between the two dots this geometry allows one to set the tunnel coupling J between the dots.

From transport spectroscopy on each individual dot, we find the following addition energies $E_C^{\text{dot1}} = e^2/C_\Sigma^{\text{dot1}} = 3.36$ meV and $E_C^{\text{dot2}} = 3.42$ meV, which correspond to total capacitances of about $C_\Sigma \cong 47$ aF. Modeling the quantum dots as electronic discs with a capacitance $C = 8\epsilon_0\epsilon_r r_e = C_\Sigma$ ($\epsilon_r \cong 12.8$ in GaAs) [1], we can estimate the dot radii to be $r_e \cong 54$ nm in good agreement with the lithographic dimensions seen in Fig. 1(a).

Using the above electron density we can estimate the number of electrons in each dot to be less than 15. From nonlinear transport measurements we find the following single level energies $\epsilon_{\text{dot1}}^* \approx 110$ μeV and $\epsilon_{\text{dot2}}^* \approx 117$ μeV. Temperature dependent measurements yield an electron temperature of $T_e \cong (118 \pm 8)$ mK [14]. Furthermore, the extrapolated width of the resonances at zero temperature is $\Gamma = (\Gamma_{lj} + \Gamma_{rj}) \cong 108$ μeV [$j = 1, 2$, see Fig. 1(b)] [1], which corresponds to a
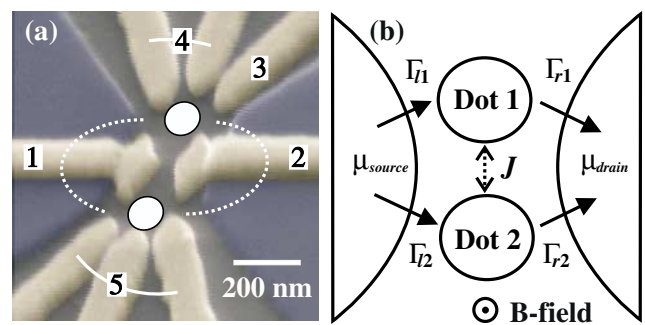
FIG. 1 (color). The device is built by electron-beam writing in a two step process. In addition to conventional Schottky gates (yellow parts) defining the quantum dots, source/drain regions are covered with a negative electron beam resist (blue areas). The circles indicate the two quantum dots within the 2DEG. (b) By applying appropriate negative voltages to the gates, a two-path quantum dot interferometer is realized. An electron in the source contact can tunnel via both dots into the drain contact. Coupling between the two dots is tuned by voltages applied to gate$_1$ and gate$_2$.

tunneling rate of $\Gamma/h \cong 2.61 \times 10^{10}$ s^{-1}. Summarizing the results so far, we find $E_C > \epsilon^*_{\text{dots}} \sim \Gamma > k_B T_e$, where charge transport is dominated by tunneling through single particle levels.

In the following section we demonstrate that the device operates as an AB interferometer: For this purpose we connect gate$_3$ and gate$_4$ and detect the source/drain current at a small source/drain bias [15]. In Fig. 2(a) the resulting charging diagram for the weak coupling regime
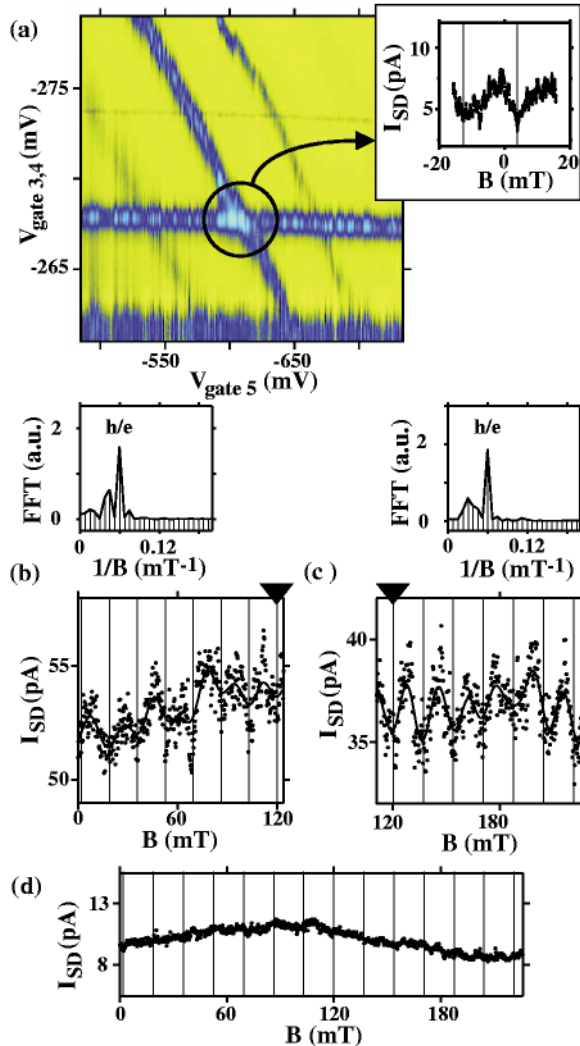
FIG. 2 (color). (a) For weak coupling we find Coulomb blockade resonances of the double dot intersecting. The device operates as an Aharonov-Bohm (AB) interferometer (yellow $\leq$ 0 pA $<$ blue $<$ 6 pA $\leq$ bright blue). If a magnetic field is applied perpendicular to the quantum dots, the amplitude of the current of the crossing points produces oscillations with a period of about $\Delta B \sim 16.4$ mT as shown in the inset. (b) and (c): On a similar sample AB oscillations are detected with a period of $\Delta B \sim 16.8$ mT. As guides to the eye black lines depict averaged curves of the measured data. The insets give the fast Fourier transformation of the oscillations. The main period corresponds to the interferometer's path as indicated by dashed lines in Fig. 1(a). (d) For only one dot in resonance to source/drain contacts and the other one in the Coulomb blockade, no oscillations are detected.

exhibits rhomboids [16]. Furthermore, the resonances intersect each other, i.e., both dots are connected to source/drain contacts. Measuring the variation of the amplitude at the crossing points of Fig. 2(a) by sweeping a perpendicular magnetic field, we detect oscillations of the current with a period of $\Delta B \approx 16.4$ mT [see inset of Fig. 2(a)]. Assuming AB interference we compute a corresponding area of $A = 2.52 \times 10^{-13}$ m^2 in corroborating accordance with the lithographic size of the two-path dot interferometer [depicted by dashed lines in Fig. 1(a)]. Following Ref. [2] we can estimate the dwell time for electrons moving coherently through both quantum dots to be $\tau_D \cong 6{-}7$ ns. This time is of the order of dwell times up to which coherent AB oscillations were found in a setup containing only one quantum dot [2]. A second similar sample shows equivalent AB oscillations which are depicted in Figs. 2(b) and 2(c). From the Fourier transformation of this data we obtain an oscillation period of $\Delta B \approx 16.8$ mT [see insets of Fig. 2(b) and 2(c)]. Furthermore, we find phase locking of the oscillations, as expected for a two terminal AB interferometer (black triangles mark the minimum at 120 mT) [17]. For comparison, the magnetic field dependence of the source/drain current for only one dot in resonance and the second dot in Coulomb blockade is shown in Fig. 2(d), i.e., the noise level is reduced and no AB oscillations can be detected.

Considering Ref. [4] we focus on the coherent coupling of the two quantum dots. As seen in transport measurements [6], coherently coupled states lead to tunnel split resonances in charging diagrams. In our experiment, this was detected by tuning V_{gate3} and V_{gate4} [18]. Naturally, via the capacitive influence of gate$_3$ and gate$_4$ on each dot we can record a charging diagram of the double quantum dot similar to Fig. 2. Figure 3(a) shows such a charging diagram for intermediate coupling of the two quantum dots [18]. For the electrostatic coupling strengths we obtain the following ratios $C_{12}/C_\Sigma^{\text{dot1}} \cong C_{12}/C_\Sigma^{\text{dot2}} = 0.37 \pm 0.08$, where C_{12} denotes the interdot capacitance [19]. As a guideline, the black line confined by two circles in Fig. 3(a) represents the electrostatic coupling of the two quantum dots. Moreover, we can extract the regions with fixed electron numbers for dot$_1$ and dot$_2$ (N_1, N_2) as depicted by black lines in Fig. 3(b).

Apart from the boundaries defined by the orthodox electrostatic model, we observe resonances which follow in parallel to the main resonances [sketched by dotted lines in Fig. 3(b)]. Furthermore, we find resonances which are "leaking" from a ground state into the Coulomb blockade regions of the phase diagram, e.g., the resonance line between the compartments $(N_1 - 2, N_2)$ and $(N_1 - 1, N_2)$ can be traced into the $(N_1 - 1, N_2 - 1)$ region [dotted-dashed line in Fig. 3(b)]. These effects correspond to higher order tunneling events, indicating strong wave function coupling of the dots [20].

In Fig. 3(b) some triple points [21] are marked by letters A, B, C, D, and E. As expected for two coherently coupled
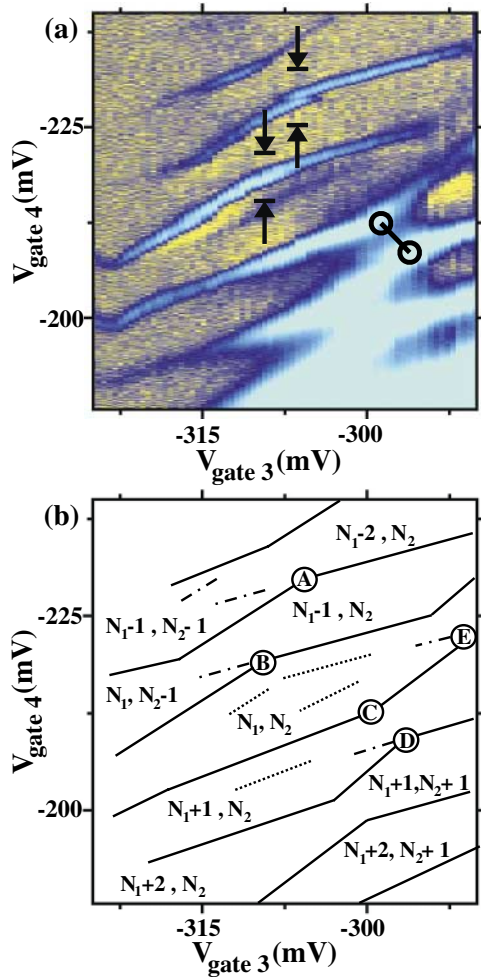
FIG. 3 (color).   (a) Charging diagram spanned by V_{gate3} and V_{gate4} in a coupling regime with strong wave function overlap in a logarithmic color scale plot (yellow $\leq$ 0 pA $<$ dark blue $<$ 6 pA $\leq$ bright blue). The black line confined by two circles denotes the electrostatic coupling of the two quantum dots. As an indication of the coherent coupling, the triple points [21] are split into two resonances (exemplarily indicated by two arrows, respectively). (b) The different compartments in the charging diagram are labeled by the electron configurations of the double quantum dot (N_1, N_2). Excited states are sketched by dashed and dotted lines, while the crossing points where the tunnel splitting occurs are marked by A, B, C, D, and E.

quantum dots, these points are tunnel split [6]. Traces crossing the split resonances are fitted by derivatives of the Fermi-Dirac distribution function with respect to V_{gate4} [see Figs. 4(a) and 4(b)] [22]. By fitting the curves in accordance with the minimum splitting [23] we can evaluate the energy difference between the two different molecular states at a triple point, respectively. We find the magnitude of the tunnel splitting varies with the triple points, i.e., the electron number in each quantum dot (e.g., for points A and B as in Fig. 4(a) we find $\Delta\epsilon_{splitA} = 132$ μeV, $\Delta\epsilon_{splitB} = 99$ μeV).

Consequentially, we recorded charging diagrams similar to the one in Fig. 3(a) applying a perpendicular magnetic
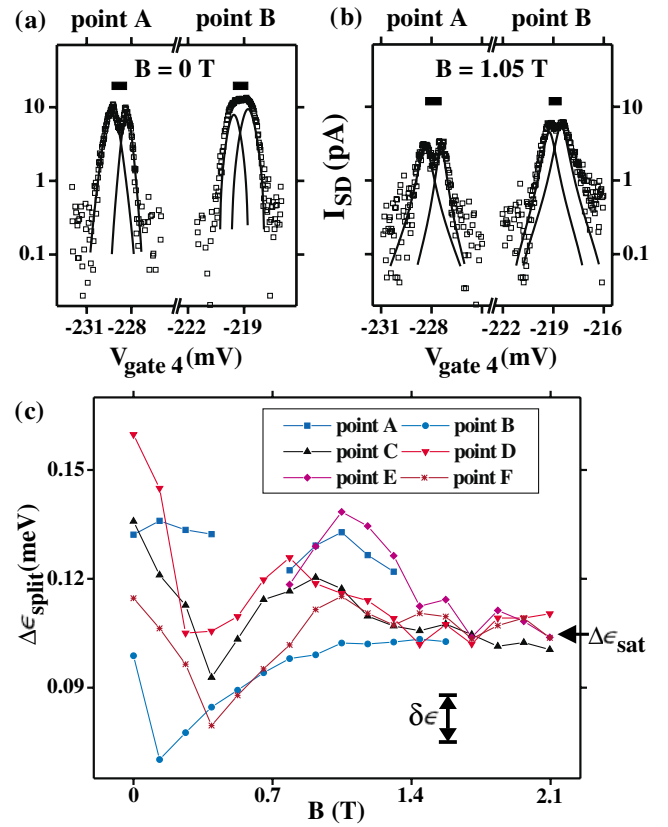
FIG. 4 (color).   (a) The logarithmic line plot shows two single traces which are indicated in Fig. 3(a) by two black arrows, respectively. The tunnel split resonances of points A and B with respect to V_{gate4} can clearly be seen (open boxes). The black lines are fits obtained with derivatives of the Fermi-Dirac distribution—the splitting δV_{gate4} is denoted by black boxes, respectively. (b) Equivalent logarithmic line plot at an applied magnetic field of $B = 1.048$ T. (c) Magnetic field dependence of the tunnel splitting $\Delta\epsilon_{split} \sim \delta V_{gate4}$. Points A to F (F out of range in Fig. 3) are the triple points [21] in Fig. 3(b). The overall error bar is indicated by $\pm\delta\epsilon = 13$ μeV.

field in the range $B = 0$ to 2 T [22]. Following the above procedure [Fig. 4(b)], we obtain a magnetic field dependence of the tunnel splitting which is depicted in Fig. 4(c). Starting with a maximum value at $B = 0$ T all curves follow a characteristic signature: Minimum around 0.12–0.4 T and a second maximum at $\sim$0.78–1.05 T. For $B > 1.4$ T we find the saturation value of the splittings to be $\Delta\epsilon_{sat} = 100$–110 μeV. We assume that both an inter-dot capacitance and an effective overlap of the wave functions have to be taken into account at the same time [9]. At zero magnetic field both contributions are superimposed. Increasing the magnetic field the two wave functions in the quantum dots are compressed and thus, their overlap is reduced. In this model the pure capacitive coupling results in an offset of about $\Delta\epsilon_{sat} \cong 110$ μeV. Below $B = 2$ T the curves resemble the magnetic field dependence of the Heisenberg exchange energy J for two excess electrons, one in each quantum dot [8]. Although the main

characteristics of all curves in Fig. 4(c) are similar, the magnitude of the splitting depends on the specific electron number. Furthermore, the trace which corresponds to the triple point B lacks a second maximum. Accordingly, we infer that the coherent coupling of the two quantum dots does not only depend on the shape of the total wave function of two coupled excess electrons as assumed so far [4], but on the specific spin and orbital electron configuration of the whole artificial molecule.

In summary, we have realized an experimental setup by which electrons can tunnel through two small quantum dots in an Aharonov-Bohm geometry, while the coupling between the dots can be broadly tuned. We demonstrate for weakly coupled dots that the setup allows one to probe Aharonov-Bohm oscillations. In an intermediate coupling regime we determine the coherent coupling of the two quantum dots and extract the magnetic field dependence of the tunnel splitting. We conclude that the whole electronic shell and spin structure have to be taken into account to describe the coherent coupling of the two artificial atoms.

---

*Email address: Alex.Holleitner@physik.uni-muenchen.de

[1] L. P. Kouwenhoven *et al.,* in *Mesoscopic Electron Transport,* edited by L. L. Sohn, L. P. Kouwenhoven, and G. Schön, NATO Advanced Study Institutes, Ser. E, Vol. 345 (Kluwer, Dordrecht, 1997).

[2] A. Yacoby, M. Heiblum, D. Mahalu, and Hadas Shtrikman, Phys. Rev. Lett. **74**, 4047 (1995); E. Buks, R. Schuster, M. Heiblum, D. Mahalu, and V. Umansky, Nature (London) **391**, 871 (1998).

[3] Y. Aharonov and D. Bohm, Phys. Rev. **115**, 485 (1959).

[4] D. Loss and E. V. Sukhorukov, Phys. Rev. Lett. **84**, 1035 (2000).

[5] D. Loss and D. P. DiVincenzo, Phys. Rev. A **57**, 120 (1998); Xuedong Hu and S. Das Sarma, Phys. Rev. A **61**, 062301 (2000).

[6] F. R. Waugh, M. J. Berry, D. J. Mar, R. M. Westervelt, K. L. Campman, and A. C. Gossard, Phys. Rev. Lett. **75**, 705 (1995); R. H. Blick, D. Pfannkuche, R. J. Haug, K. v. Klitzing, and K. Eberl, Phys. Rev. Lett. **80**, 4032 (1998).

[7] T. H. Oosterkamp, T. Fujisawa, W. G. van der Wiel, K. Ishibashi, R. V. Hijman, S. Tarucha, and L. P. Kouwenhoven, Nature (London) **395**, 873 (1998); H. Qin, A. W. Holleitner, K. Eberl, and R. H. Blick, Phys. Rev. B **64**, 241302(R) (2001).

[8] G. Burkhard, D. Loss, and D. P. DiVicenzo, Phys. Rev. B **59**, 2070 (1999).

[9] S. Nagaraja, J.-P. Leburton, and R. M. Martin, Phys. Rev. B **60**, 8759 (1999); A. Wensauer, O. Steffens, M. Suhrke, and U. Rössler, Phys. Rev. B **62**, 2605 (2000).

[10] J. Fujita, Y. Ochiai, and S. Matsui, Appl. Phys. Lett. **68**, 1297 (1996).

[11] M. Vogel (private communications); A. Tilke, M. Vogel, F. Simmel, A. Kriele, R. H. Blick, H. Lorenz, D. A. Wharam, and J. P. Kotthaus, J. Vac. Sci. Technol. B **17**, 1594 (1999).

[12] The pinch-off voltage is found to be $V_{\text{gate1}} = V_{\text{gate2}} \cong -685$ mV, whereas the presented measurements are performed at voltages of $V_{g1} = V_{g2} \geq -600$ mV.

[13] A. G. C. Haubrich, D. A. Wharam, H. Kriegelstein, S. Manus, A. Lorke, J. P. Kotthaus, and A. C. Gossard, Appl. Phys. Lett. **70**, 3251 (1997).

[14] $^{3/4}$He bath temperature was set to 50 mK.

[15] For all measurements shown the source/drain bias $eV_{\text{sd}} = \mu_{\text{drain}} - \mu_{\text{source}}$ was smaller than the single level energies ϵ^*_{dots} of the dots, i.e., for the charging diagram in Figs. 2(a) and 3(a) $eV_{\text{sd}} = -20$ μeV and for the AB curves of Figs. 2(b) and 2(c) $eV_{\text{sd}} = -50$ μeV.

[16] F. Hofmann, T. Heinzel, D. A. Wharam, J. P. Kotthaus, G. Böhm, W. Klein, G. Tränkle, and G. Weimann, Phys. Rev. B **51**, 13 872 (1995).

[17] L. Onsager, Nuovo Cimento Suppl. 2, **6**, 249 (1949); A. Ley Yeyati and M. Büttiker, Phys. Rev. B **52**, R14 360 (1995).

[18] The voltage at the two tunneling barriers which define dot$_2$ was fixed $V_{\text{gate5}} = -854$ mV.

[19] U. Wilhelm and J. Weis, Physica (Amsterdam) **6E**, 668 (2000).

[20] A. S. Adourian, C. Livermore, R. M. Westerwelt, K. L. Champman, and A. C. Gossard, Appl. Phys. Lett. **75**, 424 (1999); D. V. Averin and Yu. V. Nazarov, Phys. Rev. Lett. **65**, 2446 (1990); K. A. Matveev, L. I. Glazman, and H. U. Baranger, Phys. Rev. B **53**, 1034 (1996).

[21] A triple point denotes the position in a charging diagram where three charge configurations are degenerate.

[22] Applying a magnetic field compresses the wave functions and hence, lowers amplitude and width of the resonances. Hereby, the tunnel splitting can be more easily resolved for higher magnetic fields [see point B in Fig. 4(b) in comparison to Fig. 4(a)]. For $B > 2$ T the amplitudes of the Coulomb oscillations vanished.

[23] The maximum error of this procedure is $\pm \delta \epsilon = 13$ μeV.